Ultrasound in Medicine & Biology 000 (2023) 1–10

Contents lists available at ScienceDirect

Ultrasound in Medicine & Biology

journal homepage: www.elsevier.com/locate/ultrasmedbio

Original Contribution

Ultrasound-Induced Membrane Hyperpolarization in Motor Axons and Muscle Fibers of the Crayfish Neuromuscular Junction

Feiyuan Yu [a], Wolfgang S. Müller [a], Gösta Ehnholm [b], Yoshio Okada [c], Jen-Wei Lin [a,*]

[a] Department of Biology, Boston University, Boston, MA, USA
[b] Department of Neuroscience and Biomedical Engineering, Aalto University, Aalto, Finland
[c] Division of Newborn Medicine, Department of Pediatrics, Boston Children's Hospital and Harvard Medical School, Boston, MA, USA

ARTICLE INFO

Keywords:
Ultrasound
Crayfish neuromuscular junction
Two-pore domain potassium
Hyperpolarization

Objective: Focused ultrasound (FUS) can modulate neuronal activity by depolarization or hyperpolarization. Although FUS-evoked depolarization has been studied extensively, the mechanisms underlying FUS-evoked hyperpolarization (FUSH) have received little attention. In the study described here, we developed a procedure using FUS to selectively hyperpolarize motor axons in crayfish. As a previous study had reported that these axons express mechano- and thermosensitive two-pore domain potassium (K2P) channels, we tested the hypothesis that K2P channels underlie FUSH.

Methods: Intracellular recordings from a motor axon and a muscle fiber were obtained simultaneously from the crayfish opener neuromuscular preparation. FUSH was examined while K2P channel activities were modulated by varying temperature or by K2P channel blockers.

Results: FUSH in the axons did not exhibit a coherent temperature dependence, consistent with predicted K2P channel behavior, although changes in the resting membrane potential of the same axons indicated well-behaved K2P channel temperature dependence. The same conclusion was supported by pharmacological data; namely, FUSH was not suppressed by K2P channel blockers. Comparison between the FUS-evoked responses recorded in motor axons and muscle fibers revealed that the latter exhibited very little FUSH, indicating that the FUSH was specific to the axons.

Conclusion: It is not likely that K2P channels are the underlying mechanism for FUSH in motor axons. Alternative mechanisms such as sonophore and axon-specific potassium channels were considered. Although the sonophore hypothesis could account for electrophysiological features of axonal recordings, it is not consistent with the lack of FUSH in muscle fibers. An axon-specific and mechanosensitive potassium channel is also a possible explanation.

Introduction

Multiple non-invasive methods can be used for ablation, stimulation and modulation of neurons in the brain, including infrared, ultrasound and both electromagnetic and microwave radiation. Among these modalities, focused ultrasound (FUS) has a unique combination of attributes with promising potential for human application. FUS can stimulate or modulate focal regions of the brain through the intact skull, regardless of depth, with a focality of a few millimeters or less depending on its frequency [1,2]. A whole-head array of FUS transducers has been used to non-invasively ablate a thalamic nucleus to control essential tremor in patients [3]. Low-energy FUS safe for human use can be used to transcranially modulate neuronal activity [4,5].

Because of the wide range of possible applications for FUS in humans, there is an increasing level of interest in understanding the mechanisms of activation and modulation of neurons [6]. Sound pressures generated by FUS interact with the neuronal membrane to evoke electrophysiological events [7]. The results of mechanical perturbation of neuronal membranes include (i) activation of mechanosensitive ion channels [8–11], (ii) formation of ion-permeable lipid nanopores in the neuronal membrane [12–15], (iii) changes in membrane capacitance that are altered by either stretching or thickening of the membrane caused by intramembrane cavitation [16,17] and (iv) alterations in voltage-gated channel kinetics resulting from ultrasound-mediated changes in the lipid environment surrounding the channels [9,18,19]. These diverse mechanisms could result in either excitation or inhibition depending on which ion channels are present in a given neuron. The majority of these mechanisms result in excitation. Only two known processes, K2P channels [8,10] and cavitation that occurs intramembranously [16], can generate membrane hyperpolarization.

So far, the majority of studies involving ultrasound-mediated neuromodulation focus on the mechanisms underlying the excitation of neurons [20]. In contrast, relatively little attention has been paid to understanding mechanisms underlying ultrasound-mediated inhibition

* Corresponding author. Department of Biology, Boston University, 5 Cummington Mall, Boston, MA 02215, USA.
E-mail address: jenweilin@bu.edu (J.-W. Lin).

https://doi.org/10.1016/j.ultrasmedbio.2023.08.016
Received 30 November 2022; Revised 16 August 2023; Accepted 20 August 2023

Please cite this article as: F. Yu et al., Ultrasound-Induced Membrane Hyperpolarization in Motor Axons and Muscle Fibers of the Crayfish Neuromuscular Junction, Ultrasound in Medicine & Biology (2023), https://doi.org/10.1016/j.ultrasmedbio.2023.08.016

of neuronal activity. This article addresses the topic of FUS-mediated hyperpolarization in axons. Specifically, we examined possible roles for the K2P channels that hyperpolarize neurons.

The K2P channel family comprises a family of related K^+ channels that share a common topology whereby a channel is formed by two subunits, each of which contains two pore-lining domains [21]. This channel is constitutively active, that is, not voltage sensitive, and is thus important for setting resting membrane potential (resting V_m) or input resistance (R_{in}) [22]. Both temperature and membrane stretch have been reported to regulate the activity of the K2Ps [23,24]. K2P channels close as temperature is lowered and open as it is raised [24]. This temperature sensitivity provides a mechanism by which neurons can adapt to changes in metabolic state. By contrast, mechanosensitivity implicates this channel in sensory transduction and adaptation in situations in which neuronal swelling and shrinkage occur. Both the thermo- and mechanosensitivity of K2P channels have been investigated extensively in diverse biological systems [22,25,26]. The sensitivity of these channels to ultrasound has also been reported, mainly in heterologous expression systems [9,10]. However, their role in hyperpolarizing neurons has not been studied systematically. In the work described here, we investigated the potential role of K2P channels in producing ultrasound-induced hyperpolarization in neurons.

We used the crayfish opener neuromuscular junction in this report because K2P channels have been found in its motor axons [27]. This *ex vivo* preparation includes a single layer of muscle fibers innervated by two motor axons, 10–30 μm in diameter, one excitatory and one inhibitory. The muscle fibers, innervated by both axons, collectively open the claw of the first walking leg. This model system is one of the few preparations in which stable intracellular recordings from axon and muscle fibers can be obtained simultaneously for up to 48 h [28,29]. This exceptional stability allows for protocols that require a large number of trials and averaging [15,27,30,31]. Furthermore, the motor axons exhibit pharmacological and electrophysiological characteristics similar to those of typical mammalian neurons [32–34]. Thus, this preparation is an ideal model system for the study of cellular mechanisms underlying FUS-mediated hyperpolarization.

We first developed a procedure for consistently producing FUS-evoked hyperpolarization (FUSH) in the crayfish axons. The role of K2P channels in FUSH was then investigated in the presence of different levels of K2P channel activity mediated by changes in temperature and by channel blockers.

Methods

Preparation and solutions

Crayfish, *Procambarus clarkii*, were purchased from Niles Biological Supplies (Sacramento, CA, USA). Small animals of both sexes, 5–7 cm head to tail, were maintained in tap water at room temperature (22°C). The first walking leg was removed by autotomy and fixed with cyanoacrylate to a 60 mm plastic Petri dish. The opener axon–muscle preparation was dissected in crayfish saline. Crayfish saline includes (in mM): 195 NaCl, 5.4 KCl, 13.5 $CaCl_2$, 2.6 $MgCl_2$ and 10 Hepes, titrated to pH 7.4 with NaOH. Crayfish were handled humanely. As crayfish are invertebrate animals, their use does not require an IACUC protocol at Boston University.

Experimental configurations

Experimental configurations have been detailed in previous studies [13,15]. Briefly, two sharp electrodes in current clamp mode approached the motor axons and muscle fibers from the same distal-to-proximal direction, while the FUS transducer approached the preparation from the opposite direction. Axonal recordings provided in this article were obtained mainly from the primary branch of the excitatory axon.

Axon penetrations were performed under a 40 × /0.80 water immersion lens (LUMPlanFl/lR, Olympus, Tokyo, Japan), which was then removed to make room for the FUS transducer. The transducer was angled at 45°, and microelectrodes at 28°, to the horizontal plane. The FUS transducer was brought as close to the preparation as possible, with the lower edge of the FUS transducer cone ~1 mm from the bottom of the recording dish. The distance had been verified by digital readouts of a motorized manipulator (MP-285, Sutter Instrument, Novato, CA, USA). As the preparation is relatively small, such that the axonal arborization could easily be enclosed within the ultrasound focal area (1 × 1.4 mm^2), positioning of the transducer under visual guidance proved consistent. Meanwhile, muscle fibers are arranged symmetrically on both sides of a central ligament and form a single sheet. Central ends of the muscle fibers are attached to the ligament, and their peripheral ends are attached to the interior of a boat-shaped shell. This configuration allows muscle contractions to pull the ligament and open the claw. There is an approximately 0.1 mm space between the bottom surface of the muscle sheet and the interior side of the shell. The shell is glued to the dish on its exterior side. FUS passed through the axon–muscle preparation at 45° before it was scattered as a result of the cyanoacrylate solidifying into irregular surface contours as it bound the shell to the dish. This mechanical configuration is therefore similar to that of the *in vivo* situation, where ultrasound can pass through the axons and muscle fibers.

Experimental protocols

The investigation of potential roles for K2P channels in neuronal hyperpolarization was carried out in three phases.

Development of a procedure for consistently hyperpolarizing the axon

Optimal ultrasound intensity was determined in individual preparations, typically by starting at 0.1 MPa, and the pressure was increased gradually until FUS-evoked depolarization started to appear [13]. When a burst of FUS is applied to a motor axon with a pressure of 0.1–1 MPa, it initially produces hyperpolarization. This is followed by a depolarization when the pressure is higher than about 0.6 MPa [15,30]. The intensity at which FUS-induced depolarization was observed in less than 5% of the trials, typically between 0.3 and 0.6 MPa, was then used for that preparation in the remainder of the experiment.

Evaluation of the role for K2P channels in FUSH using temperature manipulation

Crayfish saline was circulated by a peristaltic pump at the rate of 1.5 mL/min. The saline was heated or cooled by contacting the thin plastic tubing used to feed the recording dish to a copper plate coupled to a 5 × 5 cm Peltier module (RoHS CP115035335, 150 W; CUI Devices, Lake Oswego, OR, USA). The perfusion inlet was positioned within 5 mm of the preparation such that the change in temperature at the axons was nearly instantaneous when temperature regulation was turned on. Temperature control was accomplished by manually adjusting the power supply to the Peltier. Bath temperature was monitored with a probe placed within millimeters of the preparation (Model BAT-12, Physitemp, Clifton, NJ, USA), and the temperature readout was digitized simultaneously with electrophysiological recordings. With room temperature varying between 19°C and 23°C and the peristaltic pump circulating the saline at 1.5 mL/min, this configuration allowed reliable cooling of the preparation to ~10°C and heating to 40°C. The FUS protocol used in temperature experiments involved an 80 ms burst of continuous waves (2.1 MHz). In these temperature experiments, one electrode was in the motor axon, while the second electrode was in a muscle fiber. A typical cycle included three trials: FUS alone, an AP train alone and FUS and an AP train simultaneously. There was a 10 s rest between trials. The cycle was repeated as the temperature was changed. (The effects of ultrasound on AP trains are not reported in this article.)

Evaluation of the role of K2P channels in FUSH using K2P channel blockers

Fluoxetine and norfluoxetine (Cayman) were used to block K2P channels [35]. The stock solutions for these blockers were prepared by dissolving them in dimethyl sulfoxide (DMSO) to 50 and 25 mM, respectively. Final

concentrations diluted in saline were 100 μM (fluoxetine) and 50 μM (norfluoxetine), respectively. These concentrations were five times the IC_{50} for TREK-1 channels published previously [22,36]. In these blocker experiments, we used a 2 MHz FUS transducer, which was of the same construction as that used in the temperature experiments. The ultrasound pulse pattern was composed of a train of 30 pulses delivered at 1 kHz with a duty cycle of 50%. This ultrasound delivery pattern was chosen to highlight the repetitive appearance of hyperpolarization evoked by individual FUS bursts. The FUS intensity was chosen according to the same criteria as outlined previously for temperature experiments. To monitor the effects of channel blockers on axonal input resistance, two microelectrodes penetrated a motor axon simultaneously—one for current injection and the second electrode for voltage recording. A typical cycle contained eight current steps, four hyperpolarizing and four depolarizing, to assess the input resistance and excitability of motor axons. The same current step series was repeated with and without FUS. There was a 2 s resting time between individual current steps.

FUS transducer

The construction of the ultrasound transducers used here has been detailed previously [13]. These were designed and constructed by one of us (Ehnholm). The active element of the transducer was a spherical piezo cup from Steminc Piezo (SMSF20C30F21, Steiner & Martins, Davenport, FL, USA). The piezo cup was driven by a power amplifier (LZY-22+, MiniCircuits, Brooklyn, NY, USA), which in turn was modulated by a function generator (DG1022, Rigol, Beijing, China). The cup had a diameter of 20 mm and spherical radius of 30 mm, which was also the focal length of the conical ultrasound beam from the cup. Rexolite (C-Lec Plastics, Philadelphia, PA, USA), a cross-linked polystyrene with low ultrasound absorption and a low reflection coefficient from soft tissues, was machined into a conical shape with the large end fitting exactly to the inside of the piezo cup. FUS sound waves passed through the cone to reach its tip, which was machined down to a concave sphere to increase the focus and FUS power. The tip pulled the original focal point closer to the transducer when it was submerged in saline. The Rexolite-to-saline interface formed a lens that made the focal spot smaller. As characterized previously, a focused FUS beam with a circular cross section 1 mm in diameter and at a 45° angle should project an elliptic focal image on the preparation with minor and major axes of 1 and 1.44 mm, respectively [13]. Taking into account the Rexolite impedance and duty cycle, the intensity of the spatial peak temporal average (ISPTA) of FUS at the focal point should be 0.94 mW/cm^2. This intensity is lower than the U.S. Food and Drug Administration (FDA) safety limit for applied temporal average energy level, which is <720 mW/cm^2 [37].

Electrophysiology

Two DC amplifiers (IE-210, Warner Instruments, Hamden, CT, USA) were used to perform current clamp recordings from the motor axon and a muscle fiber. Voltage signals were low-pass filtered at a cutoff frequency of 5 kHz and digitized at 50 kHz. Data were digitally sampled with a NI 6251 board (National Instruments, Austin, TX, USA) and analyzed with IGOR PRO (Wavemetrics, Lake Oswego, OR, USA). Microelectrodes for axonal recording were filled with 500 mM KCl and had a resistance of 40–60 MΩ. Microelectrodes for muscle recordings were filled with 3 M KCl and had a resistance of 10–20 MΩ. The typical resting membrane potential (V_m) of axon was ~−70 mV, and that of muscle, ~−80 mV. Each preparation represents a recording session from a motor axon dissected from an animal. A recording session typically lasted 2–4 h.

Data analysis

Statistical results presented in graphs are expressed as averages and standard errors of the mean (SEM). Statistical significance was determined with Student's *t*-tests.

Results

We first examined the role of K2P channels on FUSH by cooling, which should close the channels and thereby increase the reservoir of channels available for opening by FUS. We tested whether FUSH is specific to axons by comparing responses recorded from muscle fiber with those recorded simultaneously from motor axons. Cooling was followed by heating to test whether raised temperatures, which should open the channels, had the opposite impact on FUSH. Finally, we evaluated the potential role of K2P channels in producing FUSH by K2P blockers.

Effects of cooling on FUSH in motor axons

Figure 1 illustrates a representative experiment in which FUS-evoked responses were recorded at room temperature (24°C) first (A), followed by cooling to 15°C (B), and finally back at room temperature (23°C) (C). The ultrasound protocol was an 80 ms continuous sinusoidal burst at 0.6 MPa. At room temperature, a single FUS burst consistently triggered a small hyperpolarization. Figure 1A displays traces overlaid from individual trials (*black*) and the averaged trace (*red*). The average of FUS evoked responses at room temperature revealed a small hyperpolarization during FUS application (*black bar*) that was followed by a slow recovery (Fig. 1A, *red*). On cooling, the FUSH became stronger and clearer (Fig. 1B). The average at 15°C revealed a ~6 mV hyperpolarization during the FUS burst (*red*). On returning to room temperature, FUSH amplitudes were reduced from those recorded at 15°C (Fig. 1C) but did not return to control levels.

To ensure that the axonal properties were not adversely affected by the cooling or FUS, we monitored action potentials (APs) between FUS trials. Figure 1D illustrates APs recorded at 24°C (*black*), 15°C (*blue*) and back at 23°C (*green*), respectively. These APs are propagating action potentials evoked by a suction electrode placed proximal to the axonal recording site, ~10 mm away. Cooling depolarized resting membrane potential (V_m) of the motor axon and increased AP amplitude and duration (Fig. 1D, *black* vs. *blue*). The rightward displacement of the AP at 15°C was due to a slowing of AP conduction velocity at this low temperature. These temperature-dependent changes in AP characteristics are consistent with healthy neuronal responses reported previously that have been attributed to the temperature dependence of Na^+ and K^+ channel kinetics [38,39].

A return to the room temperature resulted in partial but stable recovery of resting V_m and AP amplitudes. Timelines of temperature changes (*red*) and resting V_m (*black*) are provided in Figure 1E. Temperature-dependent depolarization in resting V_m can be attributed to the thermosensitivity of K2P channels [22].

Figure 1F provides the timelines of AP (*blue squares*) and FUSH amplitudes (*red circles*). The FUSH amplitudes measured from individual trials were averaged potentials during FUS application. As illustrated in Figure 1A–C, FUSH amplitudes (in *red circles*) increased after cooling and then partially recovered after returning to room temperature. AP amplitude increased after cooling and partially recovered after returning to room temperature. In most preparations, AP amplitudes were fully reversible. In contrast, FUSH recovery was incomplete in all preparations, suggesting hysteresis of this parameter. Data used for statistical analysis were chosen from the period during which temperatures were in a steady state indicated by the *black bars* in Figure 1F. In this preparation, FUSH amplitudes were small but hyperpolarizing initially at room temperature (-0.7 ± 0.26 mV, $n = 17$). They were significantly larger during cooling (-6 ± 0.12 mV, $n = 30$).

Enhancement of FUSH by cooling is specific to axons

The FUSH was specific to motor axons. Figure 2 illustrates intracellular recordings from a muscle fiber obtained simultaneously with the axonal recordings in Figure 1. In this case, depolarizing deflections in V_m during FUS application exhibited stepwise changes, suggestive of FUS-

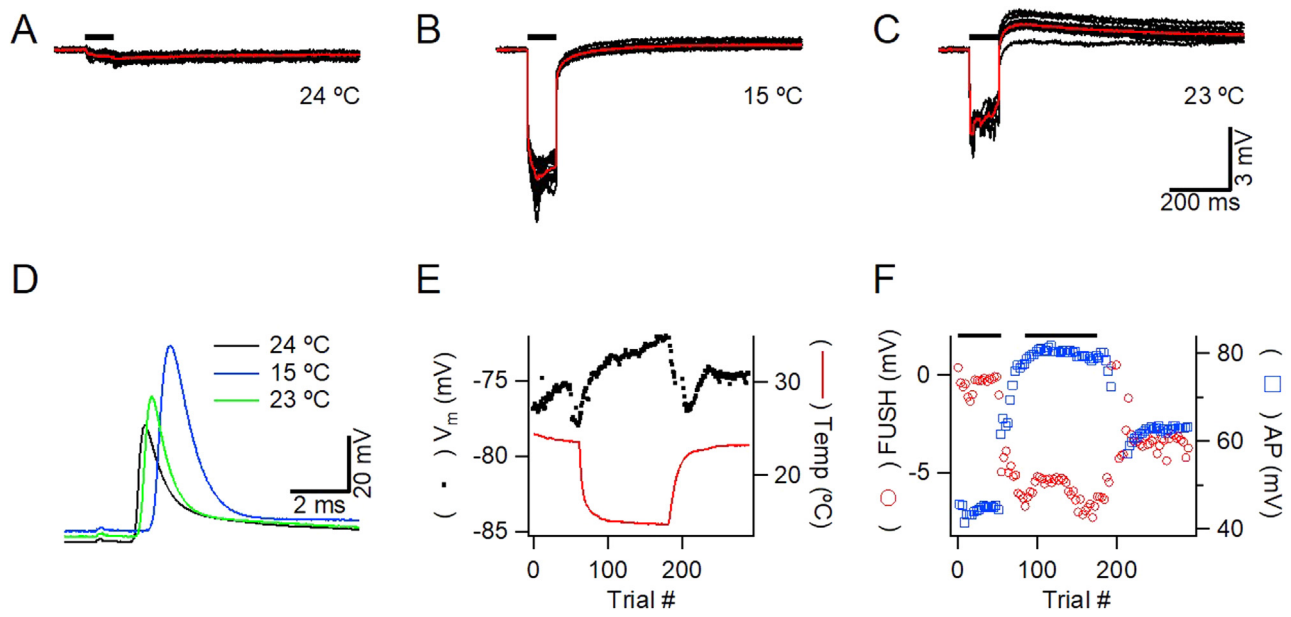

Figure 1. Effect of cooling on focused ultrasound (FUS)-induced hyperpolarization (FUSH) in a motor axon. (A) US at 2.1 MHz and 0.6 MPa with a duration of 80 ms (*black bar*) induced a small hyperpolarization at 24°C. (B) The same US tone evoked fluctuating hyperpolarization when the preparation was cooled to 15°C. (C) Reheating the preparation to control level reduced FUSH. *Black traces* in (A)–(C) are recordings from individual trials, while *red traces* represent averages. The *black bar* in (A)–(C) indicates the timing of US. The sample size used for the averages in (A), (B) and (C) were 11, 14 and 9, respectively. (A)–(C) share the same scales. (D) Action potentials (APs) recorded from the same axon as that in (A)–(C) under indicated temperatures. The AP recordings were single trials and evoked by a suction electrode. (E) Timelines of resting membrane potential (V_m, *black*) and temperature (*red*). (F) Timelines of AP amplitude (*blue squares*) and FUSH (*red circles*) to highlight the stability and consistency of the recordings. *Black bars* identify the time windows in which FUSH readings were used for statistical analysis.

evoked artifacts in the microelectrodes. The membrane potential deflections recorded during FUS application were small in amplitude and typically less than 0.5 mV (Fig. 2A–C). *Black traces* in Figure 2A–C represent individual trials, while *red traces* are averages. The integrity of muscle recordings was monitored by examining excitatory postsynaptic potentials (EPSPs) evoked by the APs of the motor axon. EPSPs, triggered by a train of 8 APs at 100 Hz, exhibited a strong facilitation, which is characteristic of this synapse. Cooling increased EPSP amplitude

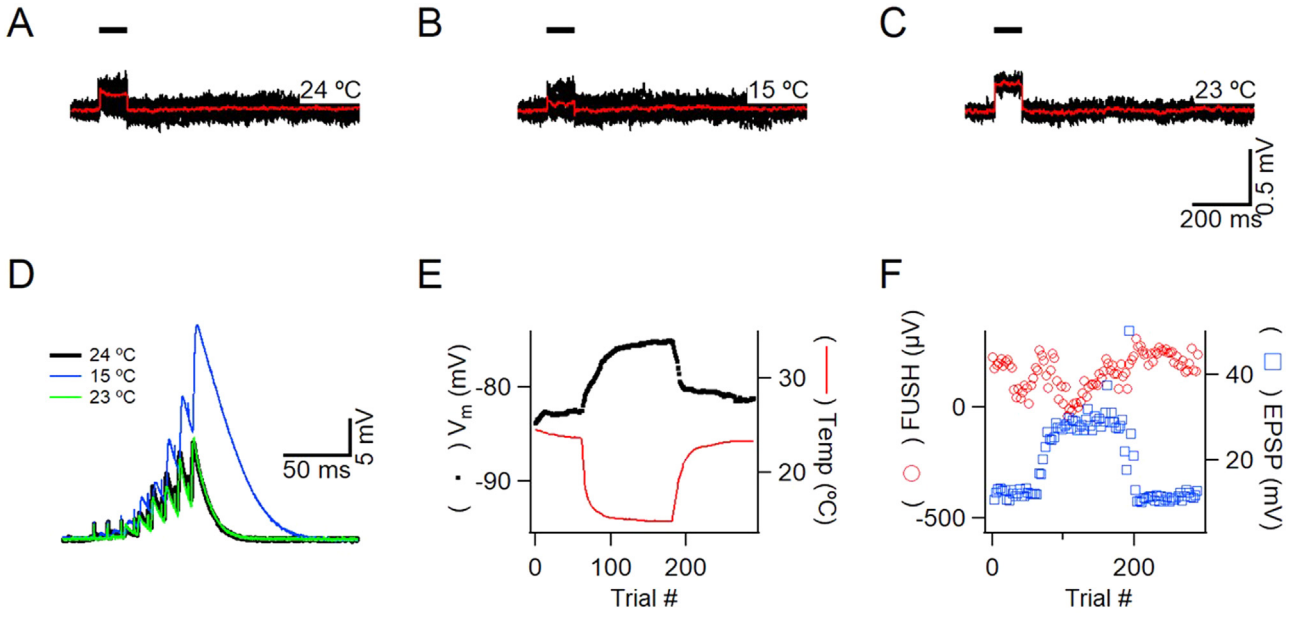

Figure 2. Cooling induced little change in focused ultrasound (FUS)-evoked responses in a muscle fiber. (A–C) Intracellular recordings from a muscle fiber obtained simultaneously from the same preparation as those in Figure 1. FUS induced small responses with step-like shapes. *Black traces* represent recordings from individual trials, and *red traces* are averages with sample sizes of 11, 14 and 9 for (A), (B) and (C), respectively. (A)–(C) share the same scale. (D) Synaptic potentials recorded under the indicated temperatures. The synaptic potentials were evoked by a train of eight APs. The excitatory postsynaptic potential (EPSP) amplitudes increased during the train because of synaptic facilitation. The EPSP traces were averages of 10, 14 and 9 trials. Baselines of EPSP traces have been aligned for comparison. (E) Timeline of resting V_m (*black*) and temperature (*red*). (F) Timelines of EPSP amplitude (*blue squares*) and focused ultrasound-induced hyperpolarization (FUSH) (*red circles*) amplitudes recorded from the muscle fiber are displayed to highlight the stability of the recordings.

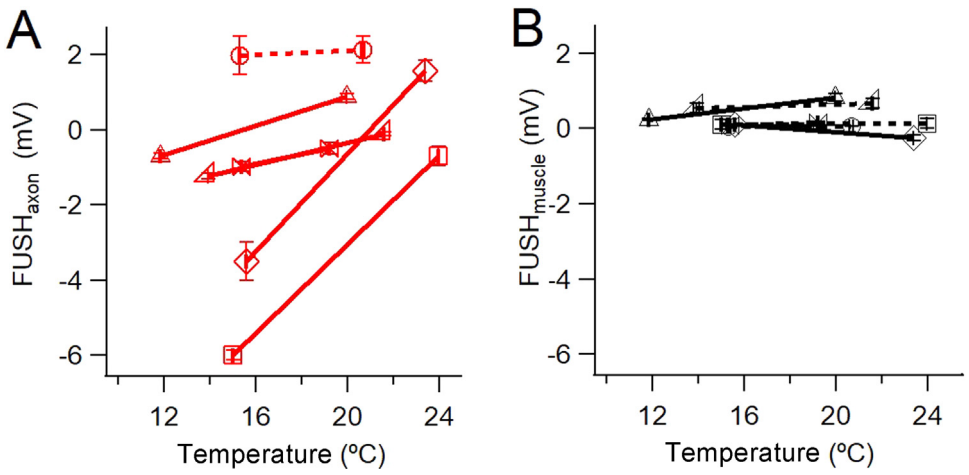

Figure 3. Summary of focused ultrasound (FUS)-induced hyperpolarization (FUSH) on cooling. (A) Average amplitudes of FUS-evoked responses in motor axons are plotted against the temperatures at which the recordings were made. Data points from the same axons are connected. Each preparation is represented by a different symbol. Error bars associated with each data point represent standard errors of the mean, but the temperature variations were typically smaller than the size of the symbols. The *dashed line* represents a preparation in which the change in FUS evoked responses was not statistically significant. Sample sizes used for average ranged from 10 to 20. (B) Average amplitudes of FUS-evoked responses recorded from muscle fibers are plotted against the temperatures from which the recordings were made. Data from the same muscle fibers are connected. Each preparation is represented by different symbols. Matching symbols in (A) and (B) mean they were obtained simultaneously from the same preparations. The *dashed lines* represent preparations for which the changes in FUS-evoked responses were not statistically significant.

(Fig. 2D, *blue*) because of the increase in amplitude and duration of presynaptic APs (Fig. 1D). EPSP baselines are aligned for comparison. Returning to room temperature restored EPSPs to their control levels (Fig. 2D, *green*). The resting V_m of the muscle fiber depolarized by 8 mV on cooling (Fig. 2E). The timeline of the EPSP maxima indicates a clear temperature dependence (Fig. 2F, *blue squares*). However, the amplitudes of FUS-evoked responses (*red circles)* recorded in the muscle fiber suggest no consistent change in FUS-evoked response amplitude as the temperature was lowered and returned to baseline. Data from the same time periods shown by the *black bars* in Figure 1F were used for statistical analysis. Amplitudes of FUS-evoked responses under control conditions were $+0.14 \pm 0.12$ mV (n = 17), and $+0.1 \pm 0.26$ mV (n = 30) during cooling. The difference in means was not statistically significant.

Summary of cooling effects on FUSH recorded in motor axons and muscle fibers

The enhancement of FUSH in motor axons with cooling was a consistent observation. Figure 3 illustrates FUSH results in six preparations for the axons (Fig. 3A) and muscles (Fig. 3B) to demonstrate the effects of temperature on FUSH across the entire set of preparations. FUSH was measured in a single axon and in a muscle fiber simultaneously. The same symbols in Figure 3A and 3B are used to show the data points obtained from the corresponding axon and muscle fiber simultaneously in the same preparations. The responses obtained during a single cooling experiment for an individual preparation are connected by a line to indicate how cooling changed the FUSH in individual axons and muscle fibers. The amplitude of FUSH was quite variable from one preparation to another, as connecting points from the same preparation brings out the consistent effect of cooling on individual preparations. In axons, five of six preparations revealed a significant increase in FUSH with cooling, whereas one preparation had a small but statistically insignificant increase during cooling (Fig. 3A, *dashed line*). A paired *t*-test of FUSH recorded at control and cooling temperature suggested that FUSH in axons was significantly increased by cooling ($p = 0.03$). In contrast to the clear FUSH signals and obvious increases in FUSH with cooling in axons, FUS-evoked changes in V_m were much smaller for muscle fibers. Changes in the FUS evoked potential with cooling were not consistent in the muscle fibers across the preparations, with four preparations exhibiting no statistically significant changes while the remaining two exhibited an increase and decrease in FUS-evoked responses, respectively.

Effects of heating on FUS-induced membrane responses in motor axons

The increase in FUSH in the axons with cooling could be due to increased activation of K2P channels by FUS. As the fraction of closed K2P channels was increased by cooling, the number of K2P channels able to be opened by a given FUS protocol would increase and enhance FUSH. If this hypothesis is correct, then we would expect decreased FUSH when the bath temperature is raised.

Figure 4 illustrates the results of a heating experiment from the same preparation used in Figures 1 and 2. Figure 4A and 4B illustrate the FUSH at room temperature and at 32°C, respectively. *Black traces* represent recordings from individual trials, while the *red traces* are the averages of the black traces. Contrary to prediction, there was no clear decrease in FUSH when the saline was heated to 32°C. As illustrated in Figure 4C, AP amplitude and duration decreased at 32°C. The leftward shift in the AP recorded after heating was due to a faster conduction velocity. These changes in AP parameters are characteristics of healthy excitable cells when temperature is raised [40,41]. Figure 4D illustrates the hyperpolarization of resting V_m on heating (*black dots*). Figure 4E illustrates the changes in FUSH (*red circles*) and AP amplitudes (*blue squares*) during the heating process. There was no clear-cut trend in FUSH amplitude with heating, although AP amplitude decreased as expected under these conditions. Averaged FUSH amplitudes in control and during heating, during the two periods represented by the horizontal bars in Figure 4E, were -3.5 ± 0.06 mV (n = 27) and -4.0 ± 0.2 mV (n = 10), respectively.

Effects of heating on FUS-evoked responses in muscle fibers

Figure 5A and 5B provide intracellular recordings from a muscle fiber obtained simultaneously with the axonal recordings in Figure 4. Similar to the muscle recordings made during cooling (Fig. 2A, 2B), deflections in V_m during FUS application exhibited stepwise shapes with small amplitudes (Fig. 5A, 5B). The integrity of muscle recordings was monitored by examining EPSPs evoked by the AP train of the motor axon. Consistent with the reduction in AP amplitude and duration during heating (Fig. 4C), EPSP exhibited a clear decrease in amplitude

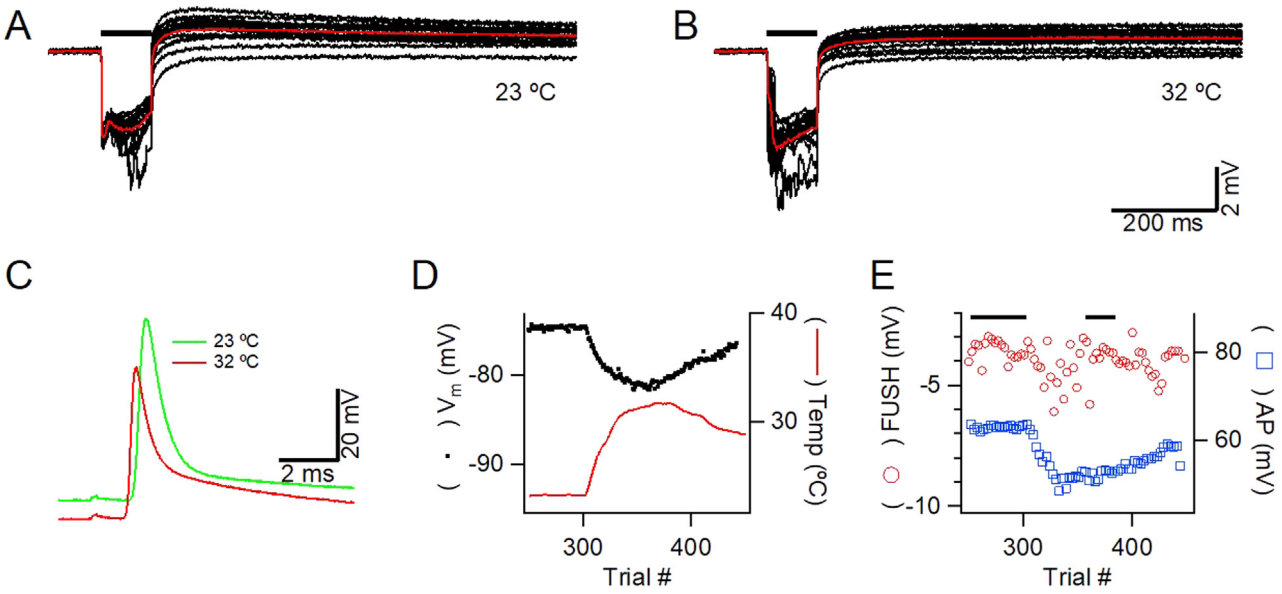

Figure 4. Effects of heating on focused ultrasound-induced responses in a motor axon. (A, B) Intracellular recordings from a motor axon as temperature was raised from 23°C (A) to 32°C (B). The heating was accompanied by a minimal change in focused ultrasound-induced hyperpolarization (FUSH) amplitude. *Black traces* in (A) and (B) are recordings from individual trials; the *red traces* are averages of displayed single trials. The sample size of the averages in (A) and (B) was 17. (A) and (B) share the same scales. (C) Increases in temperature caused membrane potential hyperpolarization and reduction in AP amplitude and duration in the axon. Leftward displacement of the action potential (AP) recorded at 32°C (*red*) was due to an acceleration of AP conduction velocity. The AP traces were from single trials. (D) Timelines of resting membrane potential (V_m, *black*) and temperature (*red*). (E) Timelines of AP amplitude (*blue squares*) of the motor axons and FUSH (*red circles*) to highlight the stability of the recordings. *Black bars* identify the time windows in which FUSH readings were used for statistical analysis.

(Fig. 5C) during heating. Heating (Fig. 5D, *red*) hyperpolarized the membrane potential of the muscle fibers (Fig. 5D, *black line*). The maximum amplitude of the EPSP (Fig. 5E, *blue squares*) decreased from about 10 to 5 mV with heating, while the FUSH amplitudes did not reveal any clear temperature dependence. In Figure 5E, FUSH amplitudes at control temperature and during heating were +0.2 ± 0.01 mV (n = 27) and +0.1 ± 0.01 mV (n = 10), respectively. The difference in means was not statistically significant.

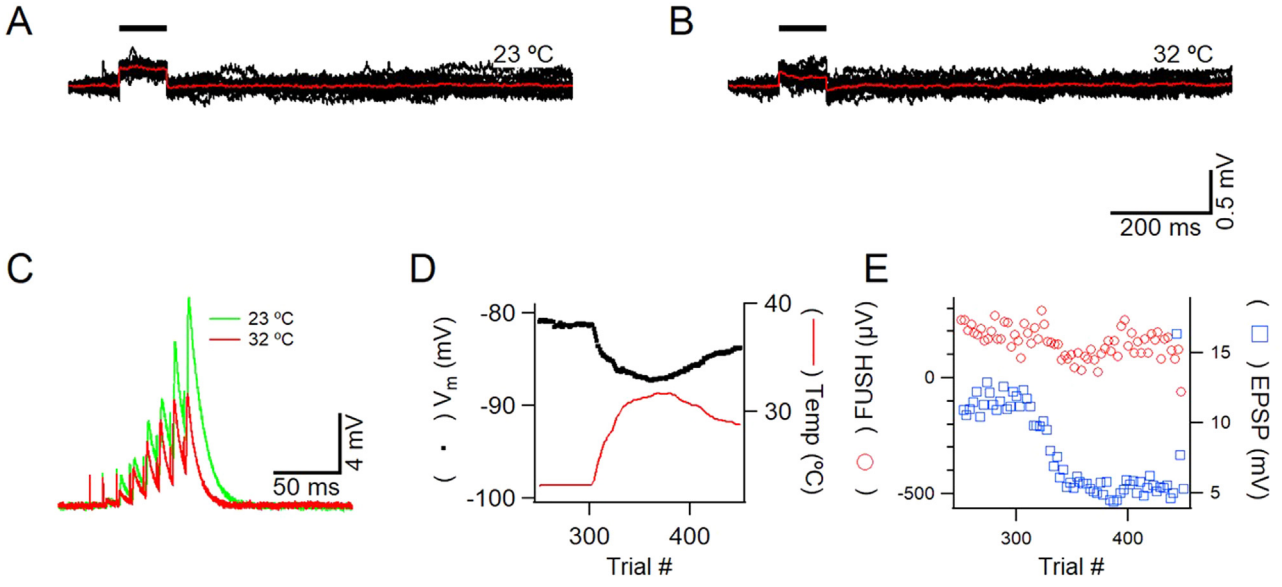

Figure 5. Heating induced little change in focused ultrasound (FUS)-evoked responses recorded from a muscle fiber. (A, B) Intracellular recordings from a muscle fiber obtained from the same preparation as those in Figure 4. FUS induced small and step-like responses. *Black traces* represent recordings from individual trials, and *red traces* are averages with sample sizes of 17 for (A) and (B). (A) and (B) share the same scales. (C) Synaptic potentials were recorded at the two temperatures shown in (A) and (B). The synaptic potentials were evoked by a train of eight action potentials (APs). Excitatory postsynaptic potential (EPSP) amplitudes increased during the train because of synaptic facilitation. EPSP traces were averages of 17 trials. Baselines of EPSP traces have been aligned for comparison. (D) Timeline of resting membrane potential (*black*) and temperature (*red*). (E) Timelines of EPSP (*blue squares*) and FUSH (*red circles*) amplitudes recorded from the muscle fiber are illustrated to highlight the stability of the recordings.

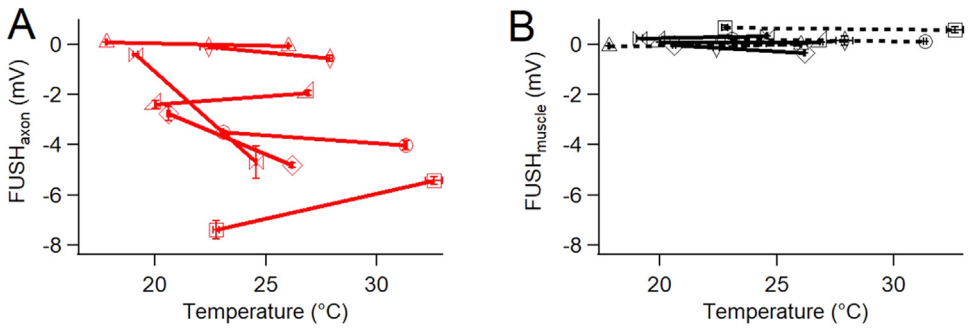

Figure 6. Summary of focused ultrasound (FUS)-induced hyperpolarization on heating. (A) Average amplitudes of FUS-evoked responses in motor axons are plotted against the temperatures at which the recordings were made. Data from the same axons are connected. Each preparation is represented by a different symbol. Sample sizes used for average ranged from 7 to 20. (B) Average amplitudes of FUS-evoked responses recorded from muscle fibers are plotted against the temperatures at which the recordings were made. Data from the same muscle fibers are connected. Each preparation is represented by different symbols. The symbols that match those in (A) mean they were obtained simultaneously in the same preparations. *Dashed lines* represent preparations for which the changes in FUS-evoked responses were not statistically significant.

Summary of heating effects on FUSH recorded in motor axons and muscle fibers

Figure 6A represents the heating effects on FUSH in seven preparations. Contrary to the prediction based on the K2P hypothesis, there was no consistent decrease in FUSH with heating. Heating the bath by nearly 10°C in some cases resulted in an increase in FUSH amplitude in two axons and a decrease in five axons. A paired *t*-test of the heating effects on FUSH amplitudes from the seven preparations indicated no statistically significant change ($p = 0.19$). Similar to the situation with cooling, FUS-evoked responses in muscle fibers, from the same preparations as those used in Figure 6A, were small, and heating did not change FUSH in any consistent direction. Of the seven preparations plotted, only three preparations showed statistically significant but small changes (Fig. 6B, *solid lines*).

Comparison of the temperature dependence of FUSH and resting V_m

As mentioned previously, we expected a consistent decrease in FUSH amplitude with heated bath temperature increase if K2P channels were responsible for FUSH. Figure 7A brings both the cooling and heating results together to illustrate the trend in FUSH amplitude as a function of bath temperature for motor axons over the entire temperature range we studied (12°C −33°C) (Figs. 3A and 6A combined). The data scattering suggests that FUSH does not decrease with temperature across the entire temperature range we studied. The linear fit gave a positive correlation coefficient of 0.42 ($p = 0.16$) for the cooling experiments (*blue line*), but the coefficient was negative (−0.37, $p = 0.19$) for the heating experiments.

In contrast to the lack of consistent correlation between FUSH and temperature, V_m measured from motor axons exhibited a continuous increase in the temperature range 12°C to 33°C (Fig. 7B). Regression analyses yielded statistically significant correlations for cooling (*blue line,* $R = -0.69$, $p = 0.013$) and heating (*red line,* $R = -0.58$, $p = 0.03$), as well as for the combination of both data sets across the entire temperature range (*gray dashed line,* $R = -0.68$, $p = 0.0001$). These results suggest that K2P channel activity increased with temperature in the motor axons, consistent with previous studies across a similar temperature range [42]. However, FUSH amplitude data do not conform to the temperature dependence expected if K2P channels played a key role in determining FUSH. Finally, the temperature dependence of resting V_m recorded from muscle fibers of the same preparations used in Figure 7A and 7B were also compiled (Fig. 7C). The data trend is similar to that derived from axons, namely, a consistent increase in V_m with rising temperature. Regression analyses of temperature dependence of muscle resting V_m revealed significant correlations for the data sets from cooling (*blue line,* $R = -0.75$, $p = 0.005$), heating (*red line,* $R = -0.58$, $p = 0.03$) or their combination (*gray dashed line,* $R = -0.72$, $p = 0.00034$). The significant temperature dependence of muscle resting V_m suggests the presence of well-behaved K2P channels. Therefore, FUSH recordings from muscle fibers, with small amplitudes and no temperature dependence, provide additional support for the argument that K2P channels do not underlie FUSH.

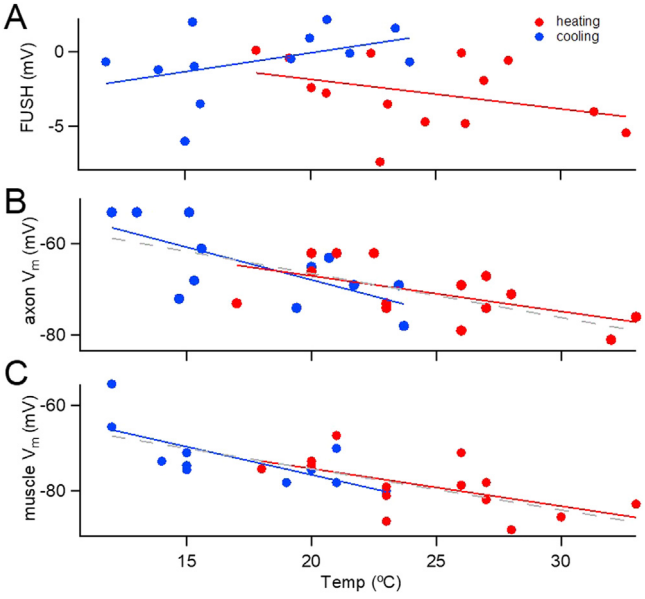

Figure 7. Compilation of focused ultrasound-induced hyperpolarization (FUSH) and resting V_m from heating and cooling experiments. (A) FUSH amplitude recorded at all temperatures, including cooling and heating. The data points were from axonal recordings in Figures 3A and 6A. The *blue line* represents a linear fit to the cooling data points, with a slope of 0.25 mV/°C. The *red line* represents a linear fit to the heating data point, with a slope of −0.2 mV/°C. Neither fit represents a statistically significant correlation. (B) Resting V_m plotted against temperature from the same axons used in (A). Color codes are the same as those in (A). The *blue line* represents a linear fit to data points collected from cooling experiment, with a slope of −1.44 mV/°C. The *red line* is calculated from fitting heating data, with a slope of −0.78 mV/°C, and the *gray dashed line* represents the linear fit to the entire data set with a slope of −0.96 mV/°C. (All resting V_m–temperature correlations were statistically significant. See text for details on statistical significance.) (C) Resting V_m plotted against temperature for muscle fibers used in Figures 3 and 6. Color codes are the same as those in (A). The *blue line* represents a linear fit to data points collected from the cooling experiment, with a slope of −1.3 mV/°C. The *red line* is calculated from fitting heating data, with a slope of −0.88 mV/°C, and the *gray dashed line* represents the linear fit to the entire data set with a slope of −0.97 mV/°C. (All resting V_m–temperature correlations were statistically significant. See text for details on statistical significance.)

Role of K2P channels in FUSH tested using pharmacological blockers

We first verified the presence of K2P channels in the crayfish motor axons using the specific K2P channel blockers fluoxetine and norfluoxetine. Figure 8A illustrates that 100 μM fluoxetine depolarized the resting V_m and increased input resistance (R_{in}). A series of current steps that evoked subthreshold membrane responses in control saline were recorded first (*black*). The membrane responses to the same current steps increased after the introduction of fluoxetine (*red*). The voltage–current relationship measured from subthreshold responses revealed a 1.8-fold increase in R_{in} after fluoxetine (Fig. 8A, inset). The membrane depolarization and increase in R_{in} resulted in AP firing triggered by a +20 nA current step, which was subthreshold before the blocker. These results confirm the presence of K2P channels in the crayfish motor axons.

We next examined whether FUSH was inhibited by fluoxetine in preparations where K2P channels block had been confirmed by the increase in R_{in}. Thirty FUS tone bursts, at 1 kHz and with 50% duty cycle, were used to trigger FUSH. This protocol was chosen to facilitate the visualization of FUSH evoked by individual tone bursts. Comparison of FUSH recorded before (*black*) and after (*red*) 100 μM fluoxetine revealed an increase in FUSH amplitude after addition of the blocker (Fig. 8B). Averages of FUSH recorded before and after fluoxetine are compared in the inset to Figure 8B, in which FUSH evoked by the first five bursts are overlaid. Figure 8C illustrates the timeline of fluoxetine effects on R_{in} and $FUSH_{pp}$. ($FUSH_{pp}$ is defined in the inset to Fig. 8B.) Fluoxetine (100 μM) was added to the bath at the time indicated by the vertical line. The addition of this blocker was followed by an increase in R_{in} (*blue squares*) and $FUSH_{pp}$ (*red circles*). The increase in FUSH in motor axons where K2P channels have been blocked suggests that this channel is unlikely to mediate FUSH.

Results obtained from fluoxetine were confirmed in a different preparation using norfluoxetine, which is a metabolite of fluoxetine but has a higher affinity for TREK-1 channels [22,36]. This antagonist increased R_{in}, but did not affect the $FUSH_{pp}$ amplitude (Fig. 8D, timeline and inset). These specific blockers were tested in four motor axons at room temperature: fluoxetine (n = 3, 100 μM), norfluoxetine (n = 1, 50 μM). In none of these cases did the K2P channel blockers inhibit FUSH. A previous study

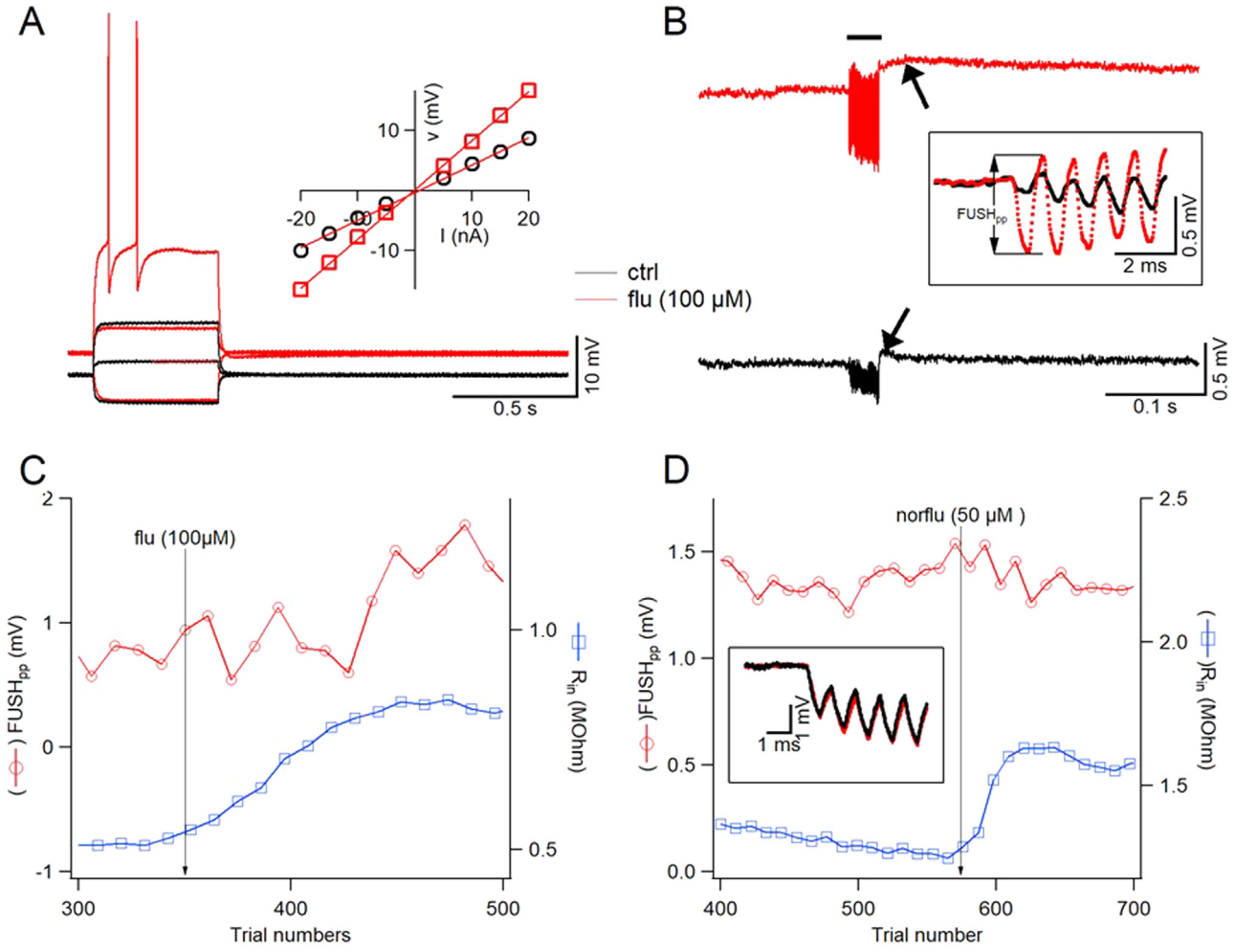

Figure 8. Effects of two-pore domain potassium (K2P) channel blockers on motor axons and focused ultrasound (FUS)-evoked responses. (A) Axonal recordings evoked by −5, +5 and +20 nA current steps. Application of 100 μM fluoxetine (*red*) caused a depolarization of resting membrane potential, by 4 mV, and an increase in input resistance such that the +20 nA step, which was subthreshold in control saline, could trigger AP firing in fluoxetine. Inset: Voltage current responses evoked by current steps from −20 to +20 nA in 5 nA increments. The input resistance increased from 0.46 to 0.81 MΩ. (B) FUS-evoked hyperpolarization recorded from the same axon as that used in (A). FUS-induced hyperpolarization (FUSH) became larger in fluoxetine (100 μM). Recordings were obtained from single trials. The *arrows* identify slight "overshoot" at the termination of FUS tone bursts. Inset: Comparison of averaged FUS-induced hyperpolarization on an expanded time scale. US induced responses evoked by individual tone bursts revealed an increase in amplitudes in fluoxetine. Individual hyperpolarization matches the duration of each FUS tone, which lasted 500 μs. FUS-evoked responses ($FUSH_{pp}$) were measured as peak-to-peak amplitudes resulting from individual 0.5 ms tone bursts. (C) Timelines of $FUSH_{pp}$ and input resistance measured from the preparation used in (A) and (B). (D) Timelines of $FUSH_{pp}$ and input resistance obtained from a different motor axon where norfluoxetine (50 μM) was used to block TREK-1 channels. The blocker effectively raised input resistance but had no impact on $FUSH_{pp}$. Inset: Averaged FUSH recordings obtained before (*black*) and after (*red*) addition of norfluoxetine. The numbers of trials used for averaging were 7 and 9, respectively.

using an infrared laser protocol to generate temperature transients has shown that K2P channels ban be blocked with Ba^{2+} (2 mM) in this preparation [31]. To verify the results obtained from fluoxetine and norfluoxetine with a non-specific blocker, we also examined the effects of Ba^{2+} in the current study. Results from using Ba^{2+} were similar to those from fluoxetine and norfluoxetine; namely, we observed an increase in R_{in}, depolarization of resting V_m and no inhibition of FUSH (n = 2). Collectively, in the six preparations we have analyzed—fluoxetine (n = 3, 100 μM), norfluoxetine (n = 1, 50 μM) and Ba^{2+} (n = 2, 2 mM)—FUSH amplitudes increased in three preparations and remained unchanged in the remaining three. As these blockers inhibited K2P channels in all preparations, evidenced by membrane depolarization and the increase in R_{in}, but did not inhibit FUSH in any of the preparations, we conclude that FUSH is unlikely to be mediated by hyperpolarizing K2P channels.

Discussion

In this study, intracellular recordings from crayfish motor axons and muscle fibers were used to examine the potential contribution of K2P channels to FUSH. FUSH was investigated under conditions where K2P channel activities could be modulated by temperature variation or pharmacological blockers. In motor axons, cooling weakly enhanced FUSH amplitude while heating suggested no temperature dependence of this parameter. As the temperature dependence of K2P channels was verified within the same axon by demonstration of temperature-sensitive changes in resting V_m, the absence of a clear temperature dependence for FUSH suggests that K2P channels are unlikely to underlie FUSH. FUS-evoked responses in muscle fibers were examined simultaneously with recordings from motor axons. FUS-evoked response in muscle fibers were small, no larger than FUS-induced electrode artifacts, and exhibited no temperature dependence. In other words, the presence of K2P channels in muscle fibers, evidenced by temperature-dependent changes in resting V_m, did not result in FUSH in those muscle fibers. Finally, K2P channel blockers were used to test whether FUSH could be inhibited by these antagonists. The blockers either had no effect or increased instead of inhibiting FUSH amplitudes, suggesting that K2P channels are unlikely to underlie FUSH. Collectively, three lines of data presented in this report suggest that mechanisms underlying ultrasound-induced membrane hyperpolarization require further investigation.

Role of K2P channels in FUSH

In neurons, K2P channels open or close in a temperature-dependent manner, which in turn determines resting V_m and R_{in} [22]. In the context of this report, FUSH enhancement by cooling could be explained by assuming that K2P channels that were closed because of the low temperature could still be opened by FUS. As a result, cooling would increase the pool of K2P channels available for opening by ultrasound [42,43]. Furthermore, the higher R_{in} at low temperatures should also increase FUSH amplitudes resulting from the opening of K2P channels. However, FUSH recorded during heating revealed no decrease in this parameter as the K2P hypothesis would predict. The absence of FUSH in muscle fibers is also consistent with the conclusion that K2P channels are unlikely to underlie FUSH. Specifically, despite the presence of K2P channels in muscle fibers, evidenced by a clear temperature dependence of muscle resting V_m (Fig. 7C), there was no detectable FUSH over the entire temperature range we tested. Finally, blocking K2P channels with both specific (fluoxetine and norfluoxetine) and non-specific (Ba^{2+}) blockers also failed to inhibit FUSH at the crayfish motor axons. Thus, our data suggest that the behavior of FUSH did not correlate with K2P channel activities that could nevertheless be manipulated by temperature or blockers. Furthermore, FUSH was absent despite the presence of K2P channels in muscle fibers. In summary, neither physiological nor pharmacological results support the K2P hypothesis. We propose that mechano- and ultrasound-sensitive potassium channels selectively present in motor axons may underlie FUSH.

Sonophore hypothesis for FUSH

In addition to ion channels, physical processes can also generate membrane hyperpolarization. It has been proposed that FUS-mediated neuromodulation could arise from an intramembranous cavitation, namely, gas bubbles forming and collapsing within the lipid bilayer (sonophore hypothesis) [16,44]. According to this hypothesis, a sinusoidal formation and collapse of bubbles increase the lipid bilayer membrane thickness at the ultrasound frequency. This increase in membrane thickness would decrease membrane capacitance, which in turn would increase V_m as long as the capacitive charges remain constant, namely, membrane hyperpolarization. Although this process has been explored by simulation [45], there has been no published experimental evaluation of this process. Our results provide some initial experimental support for this predicted mechanism of hyperpolarization. Therefore, the sonophore hypothesis appears to be a viable alternative for the generation of membrane hyperpolarization of the axons. FUSHs described in this report were typically smaller than 10 mV, a figure significantly lower than theoretical estimates of ~400 mV [45]. However, the low FUSH amplitudes reported here could be the result of filtering by the passive properties of microelectrodes. This filtering has a time resolution of ~5 kHz, while potential voltage transients resulting from intramembranous cavitation synchronized to FUS cycling at 2 MHz may be much larger. The sonophore-generated hyperpolarization at ultrasound frequency could generate inward currents, through leak channels resulting from electrochemical gradients. Cumulative effects of the inward currents could account for the overshoots that occurred at the end of the FUS burst (Fig. 8B, *arrows*). These overshoots were often observed in our recording configuration and have been noted previously [13]. Thus, the sonophore hypothesis is consistent with the characteristics of FUSH and also with electrophysiological recordings in the axons.

Difference between axon and muscle responses to FUS

Although the sonophore hypothesis can explain the FUSH data for axons, the hypothesis, at least in its simplest form, is not consistent with the effects of FUS on muscle fibers, if one assumes that such cavitation is not selective for diverse lipid compositions of different cells. We compared the effects of FUS on axons and muscle fibers by simultaneously recording the FUS-evoked responses in these cells. Although our protocol was able to clearly elicit FUSH in the axons, it did not elicit any clear FUSH in the muscle fibers. The focal area of the FUS was large enough to enclose the entire preparation. The separation between the two electrodes was 200–400 μm, which should easily be enclosed within a 1 × 1.4 mm FUS focal area. Therefore, axon and muscle recording sites are unlikely to have been subjected to different FUS pressures. Finally, it should be noted that the microelectrodes used to record from axons and muscle fibers were fabricated using the same electrode puller setting and should have identical physical characteristics. Therefore, despite the identical physical parameters used in axon and muscle recordings, FUS produced clear-cut hyperpolarization in axons, in both the cooling and heating experiments, but not in muscle fibers.

The markedly different results for axons and muscles could be due to differences in the structural organization of the lipid bilayers in these cells. In the absence of biochemical information on the respective lipid composition of axons and muscle fibers, comparison of mechanical properties attributable to the lipid composition of cell membranes are premature in the context of FUSH. Functionally, there are important differences between motor axons and muscle fibers. Motor axons have characteristics typical of excitable cells containing voltage-dependent Na^+ and K^+ channels with fast kinetics, which fire action potentials [28,33,34]. In contrast, muscle fibers at the crayfish opener neuromuscular preparation do not fire APs. Muscle contraction in this preparation is graded by the amplitude of EPSP. In addition to this difference in channel composition, muscle fibers perform force-generating contractions, while the motor axons attached to them are pulled passively.

These two modes of movement may require different types of mechanosensitive channels that support their distinct mechanical functions. The distinct assortments of voltage-sensitive and mechanosensitive channels in these two cell types could potentially provide a basis for their different capacities to manifest FUSH. Specifically, we propose that an axon-specific ultrasound-sensitive potassium channel with pharmacological properties distinct from those of K2P channels may underlie FUSH.

Conclusion

We have developed a procedure to consistently produce hyperpolarization in crayfish axons by applying focused ultrasound below a threshold pressure for producing depolarization. This enables us to study the mechanism underlying FUSH, which has received relatively little attention compared with FUS-evoked excitation. Here, we tested the hypothesis that FUSH is produced by activation of hyperpolarizing K2P channels. The role of K2P in producing FUSH was evaluated by manipulating bath temperature, which affects the activity of K2P channels, and by using K2P channel blockers. On the basis of these experimental studies, we conclude that K2P channels most probably are not the mechanism underlying FUSH. An alternative mechanism based on the concept of sonophores in the lipid bilayers may explain the FUSH observed in axons but does not explain the results for muscle fibers. The conclusions of this report suggest the need for continuing investigation of the effects of FUS on both axons and muscles, possibly by broadly exploring FUS delivery regimens and expanding the use of pharmacological and genetic tools.

Data availability statement

Primary data of this research are available on request.

Conflict of interest

The authors declare no competing interests.

Acknowledgments

This research was supported by a grant from the National Science Foundation (No. 1707865, principal investigator: Y.O.). We thank Nicky Schweitzer for editing the article.

References

[1] Baek H, Lockwood D, Mason EJ, Obusez E, Poturalski M, Rammo R, et al. Clinical intervention using focused ultrasound (FUS) stimulation of the brain in diverse neurological disorders. Front Neurol 2022;13:880814.
[2] Lescrauwaet E, Vonck K, Sprengers M, Raedt R, Klooster D, Carrette E, et al. Recent advances in the use of focused ultrasound as a treatment for epilepsy. Front Neurosci 2022;16:886584.
[3] McDannold N, Jason White P, Rees Cosgrove G. Using phase data from MR temperature imaging to visualize anatomy during MRI-guided focused ultrasound neurosurgery. IEEE Trans Med Imaging 2020;39:3821–30.
[4] Blackmore J, Shrivastava S, Sallet J, Butler CR, Cleveland RO. Ultrasound neuromodulation: a review of results, mechanisms and safety. Ultrasound Med Biol 2019;45:1509–36.
[5] Tyler WJ. Noninvasive neuromodulation with ultrasound? A continuum mechanics hypothesis. Neuroscientist 2011;17:25–36.
[6] Zhang T, Pan N, Wang Y, Liu C, Hu S. Transcranial focused ultrasound neuromodulation: a review of the excitatory and inhibitory effects on brain activity in human and animals. Front Hum Neurosci 2021;15:749162.
[7] Rabut C, Yoo S, Hurt RC, Jin Z, Li H, Guo H, et al. Ultrasound technologies for imaging and modulating neural activity. Neuron 2020;108:93–110.
[8] Douguet D, Honore E. Mammalian mechanoelectrical transduction: structure and function of force-gated ion channels. Cell 2019;179:340–54.
[9] Kubanek J, Shi J, Marsh J, Chen D, Deng C, Cui J. Ultrasound modulates ion channel currents. Sci Rep 2016;6:24170.
[10] Sorum B, Rietmeijer RA, Gopakumar K, Adesnik H, Brohawn SG. Ultrasound activates mechanosensitive TRAAK K^+ channels through the lipid membrane. Proc Natl Acad Sci USA 2021;118:e2006980118.
[11] Thompson MJ, Baenziger JE. Ion channels as lipid sensors: from structures to mechanisms. Nat Chem Biol 2020;16:1331–42.
[12] Babakhanian M, Yang L, Nowroozi B, Saddik G, Boodaghians L, Blount P, et al. Effects of low intensity focused ultrasound on liposomes containing channel proteins. Sci Rep 2018;8:17250.
[13] Lin JW, Yu F, Muller WS, Ehnholm G, Okada Y. Focused ultrasound transiently increases membrane conductance in isolated crayfish axon. J Neurophysiol 2019;121:480–9.
[14] van Wamel A, Kooiman K, Harteveld M, Emmer M, ten Cate FJ, Versluis M, et al. Vibrating microbubbles poking individual cells: drug transfer into cells via sonoporation. J Control Release 2006;112:149–55.
[15] Yu F, Muller WS, Ehnholm G, Okada Y, Lin JW. Effects of osmolarity on ultrasound-induced membrane depolarization in isolated crayfish motor axon. Ultrasound Med Biol 2022;48:2040–51.
[16] Plaksin M, Shoham S, Kimmel E. Intramembrane cavitation as a predictive bio-piezoelectric mechanism for ultrasonic brain stimulation. Phys Rev X 2014;4:011004.
[17] Prieto ML, Omer O, Khuri-Yakub BT, Maduke MC. Dynamic response of model lipid membranes to ultrasonic radiation force. PLoS One 2013;8:e77115.
[18] Lundbaek JA, Birn P, Hansen AJ, Sogaard R, Nielsen C, Girshman J, et al. Regulation of sodium channel function by bilayer elasticity: the importance of hydrophobic coupling. Effects of Micelle-forming amphiphiles and cholesterol. J Gen Physiol 2004;123:599–621.
[19] Morris CE, Juranka PF. Nav channel mechanosensitivity: activation and inactivation accelerate reversibly with stretch. Biophys J 2007;93:822–33.
[20] Blackmore DG, Razansky D, Gotz J. Ultrasound as a versatile tool for short- and long-term improvement and monitoring of brain function. Neuron 2023;111:1174–90.
[21] Sepulveda FV, Pablo Cid L, Teulon J, Niemeyer MI. Molecular aspects of structure, gating, and physiology of pH-sensitive background K2P and Kir K^+-transport channels. Physiol Rev 2015;95:179–217.
[22] Mathie A, Veale EL, Cunningham KP, Holden RG, Wright PD. Two-pore domain potassium channels as drug targets: anesthesia and beyond. Annu Rev Pharmacol Toxicol 2021;61:401–20.
[23] Kang D, Choe C, Kim D. Thermosensitivity of the two-pore domain K^+ channels TREK-2 and TRAAK. J Physiol 2005;564(Pt 1):103–16.
[24] Schneider ER, Anderson EO, Gracheva EO, Bagriantsev SN. Temperature sensitivity of two-pore (K2P) potassium channels. Curr Top Membr 2014;74:113–33.
[25] Brohawn SG. How ion channels sense mechanical force: insights from mechanosensitive K2P channels TRAAK, TREK1, and TREK2. Ann NY Acad Sci 2015;1352:20–32.
[26] Lengyel M, Enyedi P, Czirjak G. Negative influence by the force: mechanically induced hyperpolarization via K2P background potassium channels. Int J Mol Sci 2021;22:9062.
[27] Zhu X, Lin JW, Turnali A, Sander MY. Single infrared light pulses induce excitatory and inhibitory neuromodulation. Biomed Opt Express 2022;13:374–88.
[28] Lin JW. Electrophysiological events recorded at presynaptic terminals of the crayfish neuromuscular junction with a voltage indicator. J Physiol 2008;586:4935–50.
[29] Zhong N, Beaumont V, Zucker RS. Roles for mitochondrial and reverse mode Na^+/Ca^{2+} exchange and the plasmalemma Ca^{2+} ATPase in post-tetanic potentiation at crayfish neuromuscular junctions. J Neurosci 2001;21:9598–607.
[30] Lin Z, Huang X, Zhou W, Zhang W, Liu Y, Bian T, et al. Ultrasound stimulation modulates voltage-gated potassium currents associated with action potential shape in hippocampal CA1 pyramidal neurons. Front Pharmacol 2019;10:544.
[31] Zhu X, Lin JW, Sander MY. Infrared inhibition and waveform modulation of action potentials in the crayfish motor axon. Biomed Opt Express 2019;10:6580–94.
[32] Allana TN, Lin JW. Effects of increasing Ca^{2+} channel–vesicle separation on facilitation at the crayfish inhibitory neuromuscular junction. Neuroscience 2008;154:1242–54.
[33] Lin JW. Spatial variation in membrane excitability modulated by 4-AP-sensitive K^+ channels in the axons of the crayfish neuromuscular junction. J Neurophysiol 2012;107:2692–702.
[34] Lin JW. Na^+ current in presynaptic terminals of the crayfish opener cannot initiate action potentials. J Neurophysiol 2016;115:617–21.
[35] Decher N, Rinné S, Bedoya M, Gonzalez W, Kiper AK. Molecular pharmacology of K_{2P} potassium channels. Cell Physiol Biochem 2021;55(S3):87–107.
[36] Kennard LE, Chumbley JR, Ranatunga KM, Armstrong SJ, Veale EL, Mathie A. Inhibition of the human two-pore domain potassium channel, TREK-1, by fluoxetine and its metabolite norfluoxetine. Br J Pharmacol 2005;144:821–9.
[37] Miller DL. Safety assurance in obstetrical ultrasound. Semin Ultrasound CTMR 2008;29:156–64.
[38] Frankenhaeuser B, Moore LE. The effect of temperature on the sodium and potassium permeability changes in myelinated nerve fibres of *Xenopus laevis*. J Physiol 1963;169:431–7.
[39] Volgushev M, Vidyasagar TR, Chistiakova M, Yousef T, Eysel UT. Membrane properties and spike generation in rat visual cortical cells during reversible cooling. J Physiol 2000;522(Pt 1):59–76.
[40] Thompson SM, Masukawa LM, Prince DA. Temperature dependence of intrinsic membrane properties and synaptic potentials in hippocampal CA1 neurons in vitro. J Neurosci 1985;5:817–24.
[41] Trevelyan AJ, Jack J. Detailed passive cable models of layer 2/3 pyramidal cells in rat visual cortex at different temperatures. J Physiol 2002;539(Pt 2):623–36.
[42] Rueda-Ruzafa L, Herrera-Perez S, Campos-Rios A, Lamas JA. Are TREK channels temperature sensors? Front Cell Neurosci 2021;15:744702.
[43] Maingret F, Lauritzen I, Patel AJ, Heurteaux C, Reyes R, Lesage F, et al. TREK-1 is a heat-activated background K^+ channel. EMBO J 2000;19:2483–91.
[44] Lemaire T, Vicari E, Neufeld E, Kuster N, Micera S. MorphoSONIC: a morphologically structured intramembrane cavitation model reveals fiber-specific neuromodulation by ultrasound. iScience 2021;24:103085.
[45] Plaksin M, Kimmel E, Shoham S. Cell-type-selective effects of intramembrane cavitation as a unifying theoretical framework for ultrasonic neuromodulation. eNeuro 2016;3 e0136-15.2016.